

## FRAGMENTATION OF A NON-ROTATING Ni<sub>19</sub> CLUSTER: A MOLECULAR DYNAMICS STUDY

Halil Avcı and Mehmet Çivi

Department of Physics, Gazi University, Beşevler 06500 Ankara, Turkey

Ziya B. Güvenç\*

Department of Computer Engineering, Çankaya University, Yüzüncüyıl, Balgat 06530 Ankara, Turkey

Julius Jellinek

Chemistry Division, Argonne National Laboratory, Argonne IL 60439, USA

### Abstract

Collisionless fragmentation of a non-rotating Ni<sub>19</sub> cluster is studied using constant-energy molecular dynamics computer simulations. The cluster is modelled by an embedded atom model (EAM) energy surface. Distribution of the channel-specific fragmentation probabilities, and global rate constants are computed and analyzed as functions of the internal energy of the cluster. The results are compared with those obtained using the RRK statistical approach, and also compared with the other multi-channel fragmentation work.

### 1. INTRODUCTION

Structural and dynamical properties of atomic and molecular clusters are size dependent. Understanding the variation of structures and properties as clusters grow will elucidate the transition from atoms and molecules, on the one hand, and bulk matter on the other. Therefore, they are subject of increasingly intense research activity theoretically and experimentally [1-4]. Theoretical studies have been carried out for van der Waals [5-8], ionic [2] and metallic [9-10] cohesion. Further, the fragmentation of energized clusters has been the subject of a number of MD studies, however, most of them considered Lennard-Jones [5-8] system. Ejection of an atom, emerged in these studies as the only dissociation channel. In the study of fragmentation of metal clusters (M)<sub>n</sub>, n=12-14, based on many-body potential reported by Lopez and Jellinek [10], evaporation of monomers appears to be the least probable channel.

In this present work, we report results of a MD study of the collisionless fragmentation of a Ni<sub>19</sub> cluster,



The Ni<sub>19</sub> cluster was described by an EAM and fragmentation of the cluster preferentially into monomers was predicted from the simulations. In fact, fragmentation into larger products,  $i > 1$ , appears to be the least probable channels, however, there is an increasing trend for the fragmentation into larger products as the cluster energy increases. We have calculated the survival and channel specific fragmentation probabilities, and dissociation rate constants for the "super heated" Ni<sub>19</sub> cluster as functions of the cluster energy are obtained.

---

\* corresponding author. E-mail : guvenc@cankaya.edu.tr

The semi-empirical potentials used in the simulations are usually fitted to measured properties of the bulk. Some of these measured properties are indeed size dependent. Therefore the validity of the potentials will be questionable in the cluster studies. The EAM of [11] employed in this study, properties of the bulk and Ni<sub>2</sub> were used in fitting the embedding function and the pair interaction. So, one might expect that this potential could work better between the two limits i.e., range of clusters.

This work is focused on the analysis of the dynamics of the fragmentation process. In Sections 2 and 3 potential, and theoretical background and computational procedure are presented, respectively. This work is concluded with the results and discussions Section.

## 2. POTENTIAL

The cluster is described by an n-body potential (EAM), and the cohesion energy of a metallic system is obtained by the sum of the interaction energies of each of the  $n$  atoms with a host modelling the effect of the remaining  $n-1$  atoms on the one in question. The potential energy of the system is expressed as

$$V = \sum_i \left[ F_i(\bar{\rho}_i) + \frac{1}{2} \sum_{j \neq i} \phi_{ij}(r_{ij}) \right] \quad (2)$$

Where  $\bar{\rho}_i$  is the effective host electron density at the atom- $i$  site, and obtained by linear superposition of the spherically symmetric atomic density tails  $\rho_j^a$ ;

$$\begin{aligned} \bar{\rho}_i &= \sum_{j \neq i} \rho_j^a(r_{ij}), \\ \rho_j^a(r) &= r^6 (e^{-\beta r} + 2^9 e^{-2\beta r}). \end{aligned} \quad (3)$$

The  $F_i(\bar{\rho}_i)$  is the embedding energy function-energy required to embed atom- $i$  into the background electron density at site  $i$ . The  $\phi_{ij}(r_{ij})$  is a core-core, formed by the remaining charges, interaction between atoms  $i$  and  $j$  separated by a distance  $r_{ij}$ . The EAM model of Voter and Chen [11] has a medium-range attractive contribution in the core-core interaction (whereas in the version of Foiles *et al.* [12] it is entirely repulsive). But the most important change is that properties of the Ni<sub>2</sub> were used in fitting the embedding function and the pair interaction. The fit to the diatomic molecule lowers the binding energies of small Ni clusters, and results in better agreement with *ab initio* binding energies.

## 3. THEORETICAL BACKGROUND AND COMPUTATIONAL PROCEDURE

The coordinates and momenta of the atoms in the cluster are prepared starting from the zero total linear and angular momenta initial conditions. Their time evolution is generated by solving the classical equations of motion using the 4<sup>th</sup> order predictor-corrector algorithm. The time step of  $\Delta t = 4 \times 10^{-16}$  s is used in the simulation, and conservation of the total energy within 0.01% in the runs of  $4.5 \times 10^6$  steps is achieved. The quantities used to characterize the fragmentation of a cluster are, 1) channel specific fragmentation probability  $P_i$ ,

$$P_i = \frac{\tilde{N}_i}{N_0} \quad (4)$$

where  $N_0$  is the total number of trajectories that lead to fragmentation of the cluster within a specified time interval-in the simulations we had  $N_0 = 400$ . The  $\tilde{N}_i$  is the number of trajectories that result in fragmentation into channel  $i$ , i.e.,

$$N_0 = \sum_i \tilde{N}_i. \quad (5)$$

In our study the length of the maximum time interval is 1.8 ns-within this observation time all the trajectories considered in the simulations ended with fragmentation. 2) Time-dependent survival probability  $P(t)$ ,

$$P(t) = \frac{1}{N_0} \sum_{i=1}^{N_0} \theta(\tau_{0i} - t), \quad (6)$$

where  $\theta$  is the step function,  $\tau_{0i}$  is the survival time in which the cluster lives before it undergoes fragmentation along the trajectory  $i$ . 3) Global fragmentation rate constant  $k$  is defined by the equation,

$$\frac{dN(t)}{dt} = -kN(t) \quad (7)$$

where  $N(t)$  is the number of surviving parent clusters at time  $t$ ,  $N(t=0) = N_0$ . Assuming that  $k$  does not depend on time, we obtain survival probability as

$$P(t) = e^{-kt}. \quad (8)$$

The  $k$  is a function of the total energy of the cluster, and can be obtained by fitting  $\ln P(t)$  to a linear function.

Statistical model RRK (Rice-Ramsperger-Kassel) is the simplest statistical approach to unimolecular processes [13-14], which assumes that all the degrees of freedom of the system are vibrational and all are strongly coupled. It states that the system undergoes a unimolecular process when and if the energy localized in a specified vibrational degree of freedom becomes equal or larger than a certain threshold value,  $E_0$ . The rate constant  $k(E)$  of the process is proportional to the probability of such a localization and is given by [13]

$$k(E) = \nu \left[ 1 - \frac{E_0}{E} \right]^{s-1} \quad (9)$$

where  $E \geq E_0$  is the total energy of the system,  $s$  is the number of its degrees of freedom, and  $\nu$  is a frequency proportionality constant (the value of  $\nu$  is calculated as in Ref. [10]).

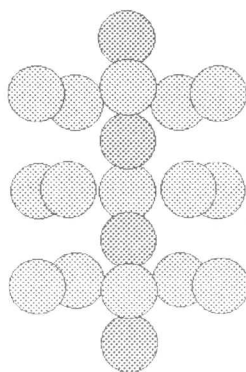


Fig. 1. Minimum energy structure of a  $Ni_{19}$  cluster. Energy per atom is  $-3.316$  eV.

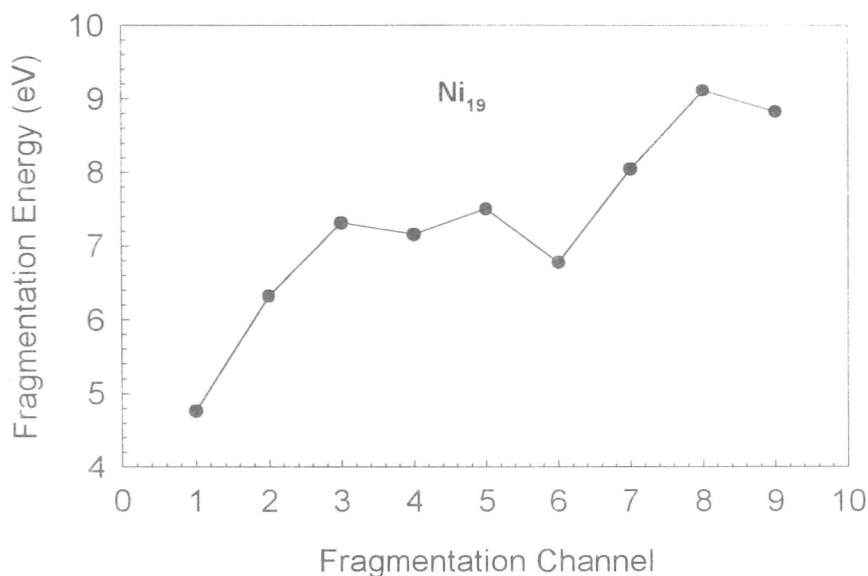


Fig. 2. Fragmentation energies of a Ni<sub>19</sub> for all possible channels

We have computed the total probabilities and rate constants at different values of the total energy of the cluster in order to analyze the energy dependence of the fragmentation. The initial conditions of the  $N_0$  number of the trajectories (coordinates and momenta) were generated and recorded every 10,000 propagation steps along the trajectory for a given total energy. Therefore, phase-space coordinates are adequate to make these initial conditions independent from each other. We have selected 5 different total energies and generated of 400 initial conditions for each total energy.

#### 4. RESULTS AND DISCUSSIONS

We had to consider energies considerably higher than the actual fragmentation energy of the cluster in order to obtain adequate statistics of the fragmentation process on the time scale of our simulations, approximately 2ns. The minimum energy geometry and the energetic of the Ni<sub>19</sub> cluster is given in Fig. 1. The fragmentation energies of the Ni<sub>19</sub> are calculated from the minimum-energy structures of the parent and fragment clusters as

$$F(i, n-i) = E(n-i) + E(i) - E(n) \quad (10)$$

where  $E(i)$ ,  $E(n-i)$ , and  $E(n)$  are the minimum energies of the parent,  $n$ , and fragment clusters  $i$ , and  $(n-i)$ , respectively. These fragmentation energies are shown in Fig. 2. Fragmentation energy is increasing first with increasing channel number  $i$ , and then, remains more less constant from the  $i=3$  to  $i=5$ . The channel  $i=6$ , which corresponds to  $Ni_{19} \rightarrow Ni_{13} + Ni_6$ , has lower fragmentation energy than the  $i=3-5$  channels since Ni<sub>13</sub> is a highly symmetric and stable cluster. The energy increases further and reaches to a maximum value at  $i=8$ . We would like to mention that the above analysis for dissociation channels is based on the total energy difference only. In actual fragmentation, the energy barriers may exist and play an important role.

The potential energy surface used in this work requires the lowest fragmentation energy for ejection of a monomer compared to the higher fragmentation channels. The next ones are the dissociation of a dimer and hexamer, respectively. In contrast, the potential energy surfaces based on the tight binding method, such as, Gupta [15] and Finnis-Sinclair

[16], favors the ejection of a dimer, i.e., requires the least energy compared to the other fragmentation channels.

Figure 3 shows the distribution of the fragmentation channel probabilities for the  $\text{Ni}_{19}$  parent cluster at five different total energies per atom. These probabilities are calculated from 400 trajectories for a given energy. The prominent feature of this distribution is that it peaks at channel  $i=1$ -ejection of a single atom. At all energies (except energy 'a') fragmentation into channel  $i \geq 2$  is observed, and their probabilities increase with increasing total energy of the cluster from "a" to "e". The channel specific probabilities for the channels  $i=3$  and 4 are quite small, therefore, error is larger and the trend is not so clear.

The global fragmentation rate constants are obtained from linear fits of the logarithms of the time-dependent survival probabilities  $P(t)$ , Eq. (6). These probabilities, as calculated from the dynamical simulations, are shown in Fig. 4. The rate of decay of the survival probabilities is indeed exponential and increases with the energy of the cluster.

In Ref. [10] the clusters  $(\text{M})_n$ ,  $n=12-14$ , were mimicked by an  $n$ -body potential that is based on Gupta's expression [15] for the cohesive energy of bulk metals. The prominent features of their results were that distributions for these sizes of the clusters peaked at channel  $i=2$ . The evaporation of monomers was practically absent and the probabilities decrease monotonically with  $i$  for  $i > 2$ . For the ranges covered, the size and the energy of the clusters seem to have no major effect on the distributions. However, our channel

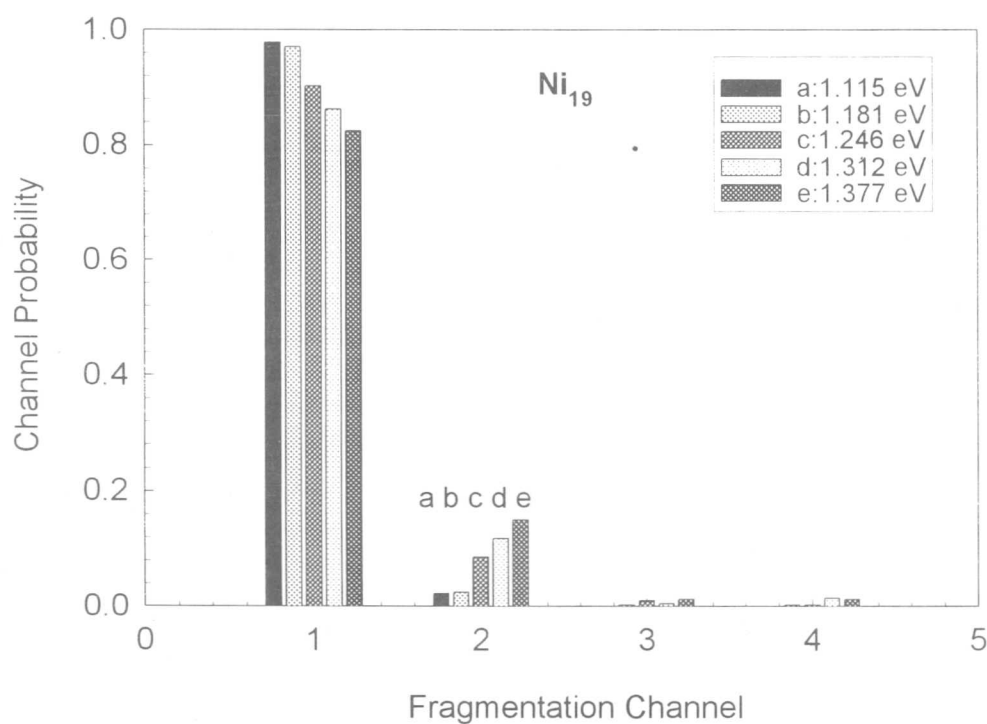


Fig. 3. Channel specific fragmentation probabilities for the  $\text{Ni}_{19}$  at different total energies per atom. The energies are defined with respect to the minimum of the potential well corresponding to its most stable geometry.

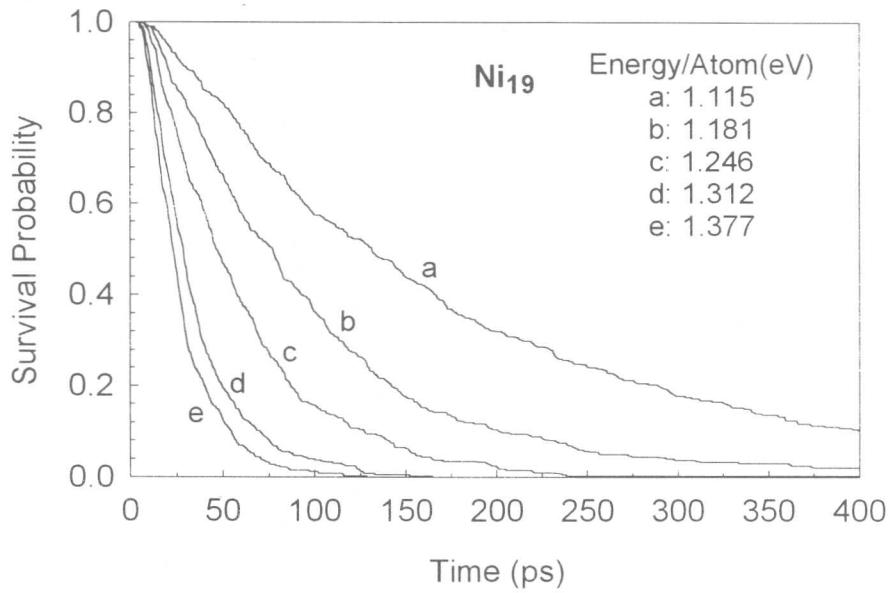


Fig. 4. Survival probability of the Ni<sub>19</sub> cluster as a function of time.

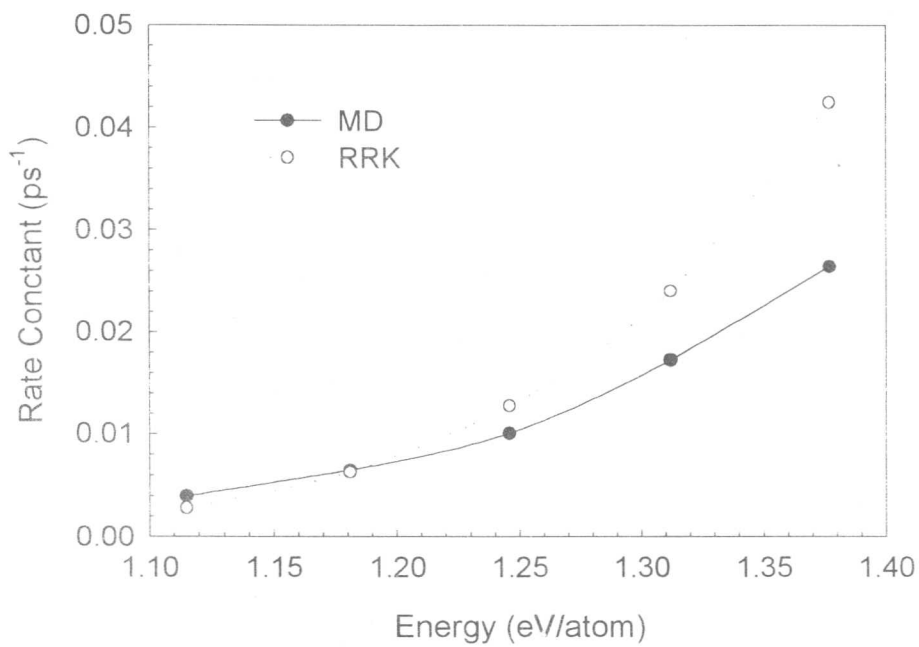


Fig. 5. Global fragmentation rate constants for the Ni<sub>19</sub> as a function of the cluster energy.

specific probabilities peaked at channel  $i=1$  and higher fragmentation channel,  $i \geq 2$ , probabilities are small. The main difference between these two simulation studies is the potential energy surfaces used. As a result, fragmentation of a cluster, as any dynamical process, depends on the topology of the potential-energy surface defining the forces acting on the atoms as well as on the total energy of the cluster.

The fragmentation energies are increasing with increasing channel number and almost reaches to a threshold value in  $i=3-5$  interval. This also correlates with the monotonic decrease of the corresponding channel probabilities. However, fragmentation into  $i \geq 5$  channels (despite the fact that the  $i=6$  has lower fragmentation energy than  $i=3-4$ ) was not observed.

As a result, there are some correlations between the fragmentation-channel probabilities, on the one hand, and the corresponding fragmentation energies, on the other.

The global fragmentation rate constants are shown in Fig. 5. The rate constants show dependence on the energy. Comparison of the results indicate that there is some correlation between the global decay rate constants obtained from the MD simulation and the statistical model RRK. However, energy dependence is stronger in RRK model than the MD (as the energy increases the difference between the two is increasing).

#### ACKNOWLEDGMENT

This work was supported by the US Department of Energy, Office of Basic Energy Sciences, Division of Chemical Sciences, Contract W-31-109-ENG-38 (JJ).

#### REFERENCES

- 1- F.G. Amar, and R.S. Berry, The onset of nonrigid dynamics and melting transition in Ar-7, *J. Chem. Phys.* **85**, 5943-5954, 1986.
- 2- R.N. Barnett, U. Landman, and G. Rajagopal, Patterns and barriers for fission of charged small metal clusters, *Phys. Rev. Lett.* **67**, 3058-3061, 1992.
- 3- Z.B. Güvenç, and J. Jellinek, and A.F. Voter, Phase changes in nickel clusters from an embedded-atom potential. In, *Physics and chemistry of finite systems: from clusters to crystals*, Kluwer Academic, Dordrecht, P. Jena, S.N. Khanna, B.K. Rao (eds), pp 411-416, 1992; and references therein.
- 4- Z. B. Güvenç and J. Jellinek, Surface Melting in Ni<sub>55</sub> Cluster, *Z. Phys.* **D26**, 304-306 1993.
- 5- F.G. Amar, and S. Weerasinghe, Is cluster evaporation statistical a comparison of simulation results for Ar-13 with exact statistical phase-space theory, *Z. Phys.* **D20**, 167-171, 1991.
- 6- C.E. Roman, and I.L. Garzon, Evaporation of Lennard-Jones clusters, *Z. Phys.* **D21**, 163-166, 1991.
- 7- C. Rey, L.J. Gallego, J. Garcia-Rodeja, M.P. Iniguez, and M.P. Alonso, A molecular-dynamic study of the evaporation of small Argon clusters, *Physica B* **179**, 273-277, 1992.
- 8- C.L. Briant, and J.J. Burton, Molecular dynamics study of the structure and thermodynamic properties of argon microclusters, *J. Chem. Phys.* **63**, 2045-2058, 1975.
- 9- I.L. Garzon, and J. Jellinek, Melting of gold microclusters, *Z. Phys.* **D20**, 235-238, 1991.
- 10- M.J. Lopez, and J. Jellinek, Fragmentation of atomic clusters, *Phys. Rev.* **A50**, 1445-1458, 1994.
- 11- A.F. Voter, and S.P. Chen, Accurate interatomic potentials for Ni, Al, and Ni<sub>3</sub>Al. In, *Symp Proc no 82. Materials Research Society*, R.W. Siegal, J.R. Weetman, R. Sinclair (eds), Pittsburg, pp 175-180, 1987.
- 12- S.M. Foiles, M.I. Baskes, and M.S. Daw, Embedded-atom-method functions for the fcc metals Cu, Ag, Au, Ni, Pd, Pt, and their alloys, *Phys. Rev.* **B33**, 7983-7991, 1986.

- 13- W. Forst, Theory of Unimolecular Reaction, Academic, New York, 1973.
- 14- R.G. Gilbert, and S.C. Smith, Theory of Unimolecular and Recombination Reactions, Blackwell Scientific, Oxford, 1990.
- 15- R.P. Gupta, Lattice-relaxation at a metal-surface, Phys. Rev. **B23**, 6265-6270, 1981.
- 16- S.K. Nayak, S.N. Khanna, B.K. Rao, and P. Jena, Physics of nickel clusters: Energetics and equilibrium geometries, J. Phys. Chem. **A101**, 1072-1080, 1997; and references therein.